




Cite this: *New J. Chem.*, 2019, 43, 14763

A FRET-based ratiometric fluorescent probe for highly selective detection of cysteine based on a coumarin–rhodol derivative†

Yu Bai,^a Ming-Xia Wu,^a Qiu-Juan Ma,^a *^a Chun-Yan Wang,^a Jing-Guo Sun,^a Mei-Ju Tian^a and Jian-Sheng Li^{*b}

Cysteine, as an important amino acid in the human body, plays a vital role in people's normal life activities. In this paper, a ratiometric fluorescent probe for detecting cysteine was designed and synthesized based on the fluorescence resonance energy transfer (FRET) process. In this FRET system, a coumarin derivative was used as the energy donor, a rhodol fluorophore was chosen as the energy receptor, and an acrylate group was utilized as a cysteine recognition unit. In the absence of cysteine, the rhodol receptor was in the non-fluorescent lactone state and the FRET process was inhibited. Upon addition of cysteine, the closed spirolactone form was converted to a conjugated fluorescent xanthene form to induce the occurrence of FRET which resulted in a fluorescent signal decrease at 470 nm and enhancement at 543 nm. The ratiometric fluorescent probe exhibited excellent selectivity to Cys over Hcy and GSH. In addition, $I_{543\text{nm}}/I_{470\text{nm}}$ of the probe for cysteine displayed a good linear relationship in the range of 5.0×10^{-7} – 1.0×10^{-4} mol L⁻¹, and the detection limit was 2.0×10^{-7} mol L⁻¹. Furthermore, the probe showed low cell toxicity and was successfully applied to the confocal imaging of cysteine in HepG2 cells using dual emission channels.

Received 28th June 2019,
Accepted 13th August 2019

DOI: 10.1039/c9nj03375k

rsc.li/njc

1. Introduction

Cysteine is an important biothiol, a common amino acid in the body, which plays an important role in reversible redox reactions, cell detoxification and metabolism.^{1,2} A high or low content of the product may cause adverse reactions in the organism. For example, the loss of cysteine leads to reduced hematopoiesis, hair pigmentation, skin development damage and cancer.^{3–6} Increased cysteine levels can cause severe neurotoxicity and cardiovascular disease.^{7–9} Therefore, the development of efficient and reliable methods for the detection of cysteine is of great significance for the early diagnosis and treatment of diseases.

The methods for detecting cysteine in recent years include high-performance liquid chromatography (HPLC),^{10,11} capillary electrophoresis (CE),^{12,13} ultraviolet-visible spectroscopy (UV-Vis),¹⁴ Fourier transform infrared (FTIR) spectrophotometry,¹⁵ and fluorescence spectroscopy.^{16,17} Among them, the fluorescent probe has the advantages of high sensitivity, good selectivity,

easy manipulation, and no damage to the test sample, and can be combined with fluorescence imaging technology for the *in situ* detection of Cys in living cells, tissues and organisms. Real-time imaging and monitoring of related biological processes have become an effective and reliable means of detection.^{18–22} Fluorescent probes currently used for cysteine often utilize the nucleophilicity of the thiol group or the high transition metal affinity of the thiol group. The detection mechanisms involve the Michael addition reaction,^{23,24} Michael addition and intramolecular cyclization reaction,^{25–28} cyclization with aldehydes,^{29,30} cleavage of sulfonamides and sulfonate esters,^{31,32} cleavage of disulfides,³³ cleavage of Se–N bonds,³⁴ metal complexes-displace coordination^{35,36} and others.^{37–39} Nevertheless, most of the reported fluorescent probes are used to detect cysteine based on fluorescence enhancement or quenching at a single emission wavelength, which may be influenced by various variable factors including excitation intensity, emission collection efficiency, probe concentration and environmental effects.^{40,41} In contrast, ratiometric fluorescent probes could be applied to resolve this problem, which can offer a built-in calibration by simultaneously measuring fluorescence intensities at two different emission wavelengths.^{42,43} The fluorescence resonance energy transfer (FRET) process is widely used in the construction of ratiometric fluorescent probes because of its large pseudo-Stokes shift and small spectral overlap, which can better distinguish the dual emission wavelengths.^{44,45} But, only

^a School of Pharmacy, Henan University of Chinese Medicine, Zhengzhou 450046, P. R. China. E-mail: maqiujuan104@126.com

^b Collaborative Innovation Center for Respiratory Disease Diagnosis and Treatment & Chinese Medicine Development of Henan Province, Henan University of Chinese Medicine, Zhengzhou 450046, P. R. China. E-mail: li_js8@163.com;

Fax: +86-371-65680028; Tel: +86-371-65676656

† Electronic supplementary information (ESI) available. See DOI: 10.1039/c9nj03375k

a few fluorescence resonance energy transfer (FRET)-based ratiometric fluorescent probes for detecting cysteine have been reported.^{46,47} Therefore, FRET-based ratiometric fluorescent probes for highly selective detection of cysteine are extremely demanded for further researching the roles of cysteine.

In this article, a FRET-based ratiometric fluorescent probe for highly selective detection of cysteine was designed and synthesized. A coumarin derivative with excellent optical properties and a high fluorescence quantum yield was used as an energy donor, a rhodol derivative was applied as an energy acceptor, and an acrylate group was utilized as a cysteine recognition group. When there is no cysteine, the rhodol energy receptor is in the non-fluorescent spirolactone form and the FRET process of the probe remains off. So, the free probe displays the inherent blue fluorescence of the coumarin chromophore. However, in the presence of cysteine the probe undergoes a Michael addition and intermolecular cyclization reaction, and the closed spirolactone form was converted to a conjugated fluorescent xanthene form to trigger the occurrence of FRET which resulted in a fluorescent signal decrease at 470 nm and enhancement at 543 nm. The ratiometric fluorescent probe exhibited high selectivity toward cysteine over Hcy and GSH. Moreover, the probe showed low cell toxicity and was successfully applied to the confocal imaging of cysteine in HepG2 cells using dual emission channels.

2. Experimental

2.1. Materials and instruments

4-(Diethylamino)salicylaldehyde, diethyl malonate, *m*-diphenol, phthalic anhydride, trifluoroacetic acid, 4-diaminopyridine (DMAP), and acryloyl chloride were purchased from Heowns Biochemical Technology Company. 1-Ethyl-3-(3-dimethylamino-propyl)carbodiimide hydrochloride (EDC) and *m*-hydroxyphenyl-piperazine were purchased from Energy Chemical (Shanghai, China). Cysteine (Cys) and homocysteine (Hys) were purchased from TCI (Shanghai) Development Company. Glutathione (GSH) was purchased from Aladdin Reagent Company. Threonine (Thr), leucine (Leu), methionine (Met), valine (Val), phenylalanine (Phe), serine (Ser), asparagine (Asn), tryptophan (Trp), tyrosine (Tyr), glutamine (Gln), lysine (Lys), isoleucine (Ile), alanine (Ala), histidine (His), aspartic acid (Asp), arginine (Arg), proline (Pro), glutamic acid (Glu) and glycine (Gly) were obtained from Shanghai Lanji Science and Technology Development Company. Anhydrous aluminum chloride and *n*-hexane were purchased from Tianjin Sailboat Chemical Reagent Technology Company. Nitrobenzene was purchased from Tianjin Damao Chemical Reagent Factory. Hexahydropyridine was purchased from Shanghai Pharmaceutical Reagent Company of China Pharmaceutical Group. Triethylamine was purchased from Tianjin Fuchen Chemical Reagent Factory. The solvents used in the high performance liquid chromatography (HPLC) experiments were all chromatographically pure and purchased from Tianjin Siyou Fine Chemicals Company. All other chemical reagents were analytically pure reagents, purchased from commercial suppliers and used directly in the experiment without further purification. Thin layer chromatography was performed

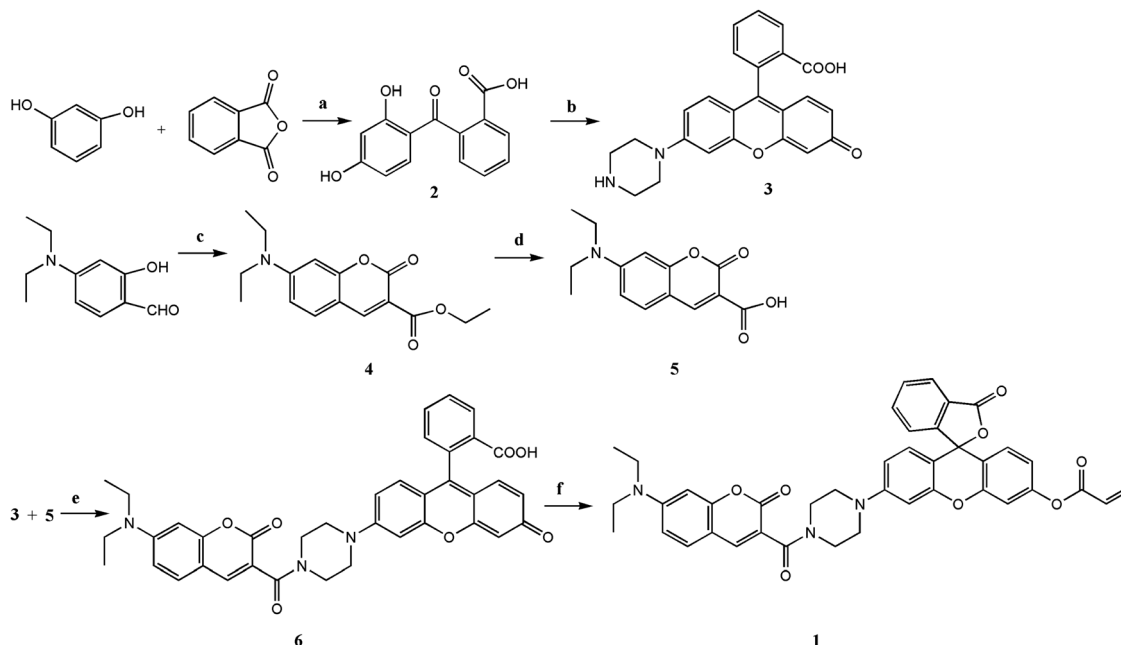
using silica gel 60 F254, and column chromatography was conducted on silica gel (200–300 mesh), both of which were purchased from China Qingdao Ocean Chemical. Water is purified using an SZ-93 automatic double pure water distiller (Shanghai Yarong Biochemical Instrument Factory).

The NMR spectrum was recorded with Bruker's DRX-500 spectrometer using tetramethylsilane (TMS) as an internal standard. Mass spectra were obtained on an Agilent Technologies 6420 Triple Quad LC/MS high resolution mass spectrometer. All fluorescence tests were performed on a Hitachi F-7000 fluorescence spectrophotometer with a 1 cm quartz absorption cell with an excitation wavelength of 418 nm and an entrance and exit slit of 10 nm. The UV-visible absorption spectrum was measured using an EVOLUTION 260 BIO UV-Vis spectrophotometer with a 1 cm quartz absorption cell. The pH was measured using a pH meter (METTLER TOLEDO Fiveeasy Plus). A DF-101S collector-type constant-temperature heating magnetic stirrer produced by Gongyi City Yuhua Instrument Company and an MS-PB magnetic stirrer manufactured by Shanghai Yuhuai Instrument Company were used in the synthesis process. High performance liquid chromatograms were obtained with an UltiMate 3000 high performance liquid chromatograph equipped with an XBP-C18 column (5 μ m, 4.6 \times 250 mm). Fluorescence images of living cells were recorded using an Olympus FV-1200 single photon laser confocal microscope. Data processing is mainly performed using SigmaPlot software. The data obtained by fluorescence spectrophotometry and UV-visible spectrophotometry were measured in 0.01 mol L⁻¹ PBS buffer (CH₃CN/water = 6 : 4, v/v, pH = 7.40). In addition to the fluorescence data obtained by time scanning, all other fluorescence and absorption data were recorded at 60 min after the addition of cysteine at room temperature.

2.2. Syntheses

The synthetic route to FRET-based ratiometric fluorescence probe **1** for highly selective detection of cysteine is shown in Scheme 1. The probe **1** uses a coumarin–rhodol fluorescence resonance energy transfer system as a mechanism. The fluorescence emission spectrum of the coumarin energy donor (compound **5**) efficiently overlaps with the UV-Vis absorption spectrum of the rhodol energy acceptor (compound **3**), indicating that the FRET process would occur to induce the appearance of acceptor emission concomitant with the disappearance of donor emission (Fig. 1).

Synthesis of compound 2. The compound **2** is synthesized according to a reported document.⁴⁵ Under a nitrogen stream, resorcinol (0.55 g, 5 mmol) and phthalic anhydride (0.74 g, 5 mmol) were dissolved in 30 mL of nitrobenzene, then anhydrous AlCl₃ (1.47 g, 11 mmol) was added, and the reaction mixture was stirred at room temperature for 12 h. The reaction mixture was poured into a two-phase solution of vigorously stirred 30 mL *n*-hexane and 40 mL 0.5 M HCl. After the reaction mixture was stirred for 2 h, an orange-yellow precipitate was obtained and filtered to give a crude product. Then the product was purified through a column chromatograph using dichloromethane/methanol (15 : 1, v/v) as the eluent to obtain



Scheme 1 Synthesis of FRET-based ratiometric fluorescent probe **1**: (a) nitrobenzene, anhydrous AlCl_3 , 84%; (b) *m*-hydroxyphenylpiperazine, CF_3COOH , 75%; (c) diethyl malonate, hexahydropyridine, 81%; (d) (I) NaOH, (II) HCl, 75%; (e) EDC, DMAP, 43%; (f) anhydrous CH_2Cl_2 , triethylamine, acryloyl chloride, 61%.

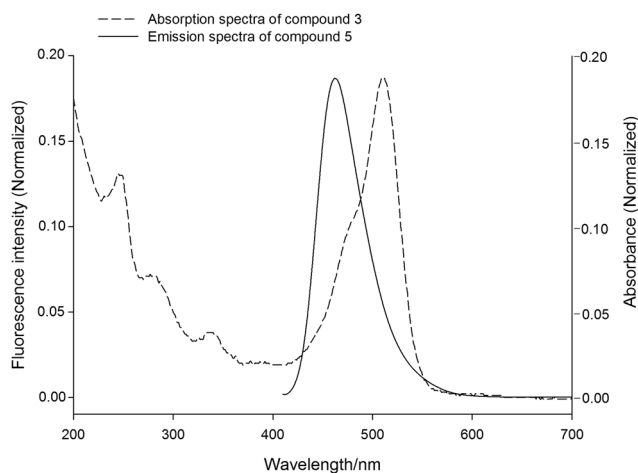


Fig. 1 Normalized emission spectra of donor derivative **5** ($5.0 \mu\text{M}$) and normalized absorption spectra of acceptor **3** ($5.0 \mu\text{M}$) in 0.01 M PBS buffer ($\text{CH}_3\text{CN}/\text{water} = 6:4$, v/v, pH = 7.40). The dashed (---) and solid line (—) represent the normalized absorption of compound **3** and normalized emission spectra of compound **5**, respectively.

compound **2** as an orange solid (1.08 g, 84%). $^1\text{H NMR}$ (500 MHz, CD_3OD), δ (ppm): 8.06 (1H, d, $J = 7.7 \text{ Hz}$), 7.65 (1H, t, $J = 7.5 \text{ Hz}$), 7.59 (1H, t, $J = 7.5 \text{ Hz}$), 7.34 (1H, d, $J = 7.5 \text{ Hz}$), 6.93 (1H, d, $J = 8.8 \text{ Hz}$), 6.31 (1H, d, $J = 2.0 \text{ Hz}$), 6.21 (1H, dd, $J = 8.8 \text{ Hz}$, 2.0 Hz).

Synthesis of compound 3. The compound **3** is synthesized according to a reported document.⁴⁵ Compound **2** (1.03 g, 4 mmol) was dissolved in 20 mL of CF_3COOH and then *m*-hydroxyphenylpiperazine (0.71 g, 4 mmol) was also added into the above mixture. This reaction mixture was heated to reflux for 36 h,

and then the solvent was removed under reduced pressure. It was further purified by column chromatography using dichloromethane/methanol (5:1, v/v) to obtain a red solid compound **3** (1.21 g, 75%). $^1\text{H NMR}$ (500 MHz, $\text{DMSO}-d_6$), δ (ppm): 10.22 (1H, s), 7.99 (1H, d, $J = 7.7 \text{ Hz}$), 7.80–7.77 (1H, m), 7.72–7.69 (1H, m), 7.24 (1H, d, $J = 7.6 \text{ Hz}$), 6.89 (1H, d, $J = 2.3 \text{ Hz}$), 6.76 (1H, dd, $J = 8.9 \text{ Hz}$, 2.3 Hz), 6.68 (1H, s), 6.58–6.55 (3H, m), 3.44 (4H, d, $J = 5.3 \text{ Hz}$), 3.21 (4H, d, $J = 4.8 \text{ Hz}$).

Synthesis of compound 4. Compound **4** was synthesized according to the reported literature.⁴⁵ 4-(Diethylamino)salicylaldehyde (0.97 g, 5 mmol) was dissolved in 25 mL $\text{CH}_3\text{CH}_2\text{OH}$, and then diethyl malonate (0.96 g, 6 mmol) and 0.5 mL hexahydropyridine were added. The reaction mixture was stirred under reflux for 2 h, diluted with 50 mL water, extracted with ethyl acetate (50 mL \times 3), and dried over anhydrous MgSO_4 . The solvent was removed under reduced pressure and the crude product was purified by column chromatography using petroleum ether/ethyl acetate (3:1, v/v) to get an orange compound **4** (1.16 g, 81%). $^1\text{H NMR}$ (500 MHz, CDCl_3), δ (ppm): 8.40 (1H, s), 7.33 (1H, d, $J = 8.9 \text{ Hz}$), 6.57 (1H, dd, $J = 8.9 \text{ Hz}$, 2.2 Hz), 6.43 (1H, d, $J = 2.1 \text{ Hz}$), 4.34 (2H, q, $J = 7.1 \text{ Hz}$), 3.42 (4H, q, $J = 7.1 \text{ Hz}$), 1.36 (3H, t, $J = 7.1 \text{ Hz}$), 1.20 (6H, t, $J = 7.1 \text{ Hz}$).

Synthesis of compound 5. Compound **5** was synthesized according to the reported literature.⁴⁵ Compound **4** (1.05 g, 4 mmol) was dissolved in 40 mL ethanol and then 40 mL 0.5 M NaOH was added. This mixture was stirred at room temperature for 12 h. The solvent was evaporated under reduced pressure to give a solid. The solid was dissolved in 5 mL water, and the solution was acidified with 1 M HCl to give a precipitate. When the precipitate was filtered, a red-brown solid compound **5** (0.78 g, 75%) was obtained. $^1\text{H NMR}$ (500 MHz,

CDCl_3 , δ (ppm): 12.30 (1H, s), 8.64 (1H, s), 7.44 (1H, d, $J = 9.1$ Hz), 6.69 (1H, dd, $J = 9.1$ Hz, 2.4 Hz), 6.51 (1H, d, $J = 2.4$ Hz), 3.47 (4H, q, $J = 7.2$ Hz), 1.24 (6H, t, $J = 7.2$ Hz).

Synthesis of compound 6. Under nitrogen protection, compound 3 (0.40 g, 1 mmol) was dissolved in 60 mL anhydrous dichloromethane/anhydrous *N,N*-dimethylformamide (5:1, v/v). Then DMAP (0.06 g, 0.5 mmol) and EDC (0.19 g, 1 mmol) were added. Then the mixture was stirred at room temperature for 30 min. Compound 5 (0.31 g, 1.2 mmol) was added and stirred overnight. The reaction solution was evaporated under reduced pressure to give a crude product. Then it was further purified by column chromatography using dichloromethane/methanol (20:1, v/v) as the eluent to get a red compound 6 (0.28 g, 43%). $^1\text{H NMR}$ (500 MHz, $\text{DMSO}-d_6$), δ (ppm): 10.10 (1H, s), 8.00–7.97 (2H, m), 7.77 (1H, d, $J = 7.5$ Hz), 7.71 (1H, d, $J = 7.5$ Hz), 7.49 (1H, d, $J = 8.9$ Hz), 7.25 (1H, d, $J = 7.6$ Hz), 6.81 (1H, s), 6.74 (2H, d, $J = 9.0$ Hz), 6.66 (1H, s), 6.54 (4H, d, $J = 7.0$ Hz), 3.69 (2H, s), 3.45–3.42 (6H, m), 3.32 (2H, d, $J = 1.1$ Hz), 3.25 (2H, s), 1.12 (6H, t, $J = 7.0$ Hz). MS (ESI) m/z : 644.1000 ($\text{M} + \text{H}$) $^+$, 666.1000 ($\text{M} + \text{Na}$) $^+$.

Synthesis of compound 1. Compound 6 (0.64 g, 1 mmol) was dissolved in 20 mL anhydrous dichloromethane followed by the addition of 1.4 mL triethylamine, then acryloyl chloride (0.18 g, 2 mmol) was added slowly. After half an hour of reaction at 0 °C, the reaction mixture was stirred at room temperature for 12 h. Subsequently, the solvent was evaporated under reduced pressure. The crude product was further purified by column chromatography using dichloromethane/methanol (30:1, v/v) as the eluent to obtain a yellow compound 1 (0.43 g, 61%). $^1\text{H NMR}$ (500 MHz, CDCl_3), δ (ppm): 7.98 (1H, d, $J = 7.6$ Hz), 7.86 (1H, s), 7.64 (1H, t, $J = 7.4$ Hz), 7.58 (1H, t, $J = 7.4$ Hz), 7.27 (1H, d, $J = 8.8$ Hz), 7.15 (1H, d, $J = 7.6$ Hz), 7.08–7.07 (1H, m), 6.80–6.76 (2H, m), 6.68 (1H, d, $J = 1.9$ Hz), 6.64–6.56 (4H, m), 6.44 (1H, d, $J = 1.9$ Hz), 6.28 (1H, dd, $J = 17.3$ Hz, 10.5 Hz), 6.01 (1H, d, $J = 10.5$ Hz), 3.86 (2H, s), 3.54 (2H, s), 3.40 (4H, q, $J = 7.0$ Hz), 3.30 (4H, d, $J = 16.6$ Hz), 1.19 (6H, t, $J = 7.0$ Hz). $^{13}\text{C NMR}$ (125 MHz, CDCl_3), δ (ppm): 169.29, 165.02, 163.88, 159.09, 157.26, 152.90, 152.52, 152.12, 151.94, 151.71, 151.69, 145.39, 135.00, 133.17, 129.86, 129.72, 128.95, 128.70, 127.45, 126.50, 124.94, 123.96, 117.11, 116.82, 115.76, 112.33, 110.17, 109.35, 109.21, 107.66, 102.35, 96.83, 82.60, 48.40, 47.95, 46.77, 44.87, 41.88, 12.33. MS (ESI) m/z : 698.2000 ($\text{M} + \text{H}$) $^+$, 702.2000 ($\text{M} + \text{Na}$) $^+$. In the DEPT135 spectrum, the chemical shift of 82.60 corresponds to the carbonyl carbon of spirolactone, indicating that compound 1 was in the spirolactone form.

2.3. Cytotoxicity assay

Cytotoxicity is an important indicator of the performance of fluorescent probes in bioimaging applications. In order to detect the cytotoxicity of the probe, the 3-(4,5-dimethylthiazole-2)-2,5-diphenyltetrazolium bromide (MTT) colorimetric method was used. The selected cells were HepG2 cells (liver cancer cells). First, the HepG2 cells were cultured in 10% fetal bovine serum medium, about 1×10^4 cells were seeded in each well of a 96-well plate and the total volume per well was controlled at 100 μL . After the HepG2 cells were placed in an incubator containing 5% CO_2 at 37 °C for 24 h, the medium was aspirated.

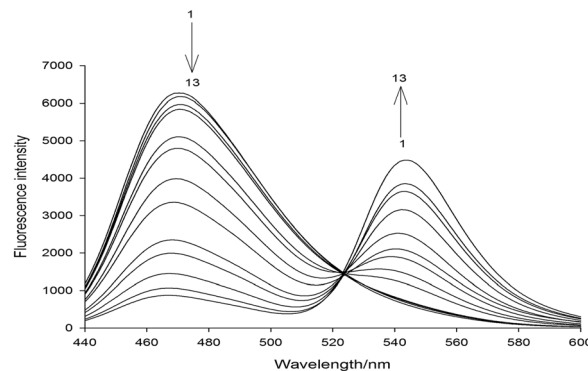


Fig. 2 One-photon fluorescence spectra of probe 1 (10.0 μM) in the presence of various concentrations of cysteine: 0, 0.5, 0.7, 1.0, 3.0, 5.0, 7.0, 10, 20, 30, 50, 70, and 100 μM from 1 to 13 ($\lambda_{\text{ex}} = 418$ nm).

Then, the HepG2 cells were incubated with different concentrations of compound 1 and compound 6 in fresh medium for 4 h. After that, the medium was removed from this 96-well plate and a fresh medium was added for 24 h. The HepG2 Cells were incubated with the fresh medium (100 μL) containing MTT (10 μL , 5 mg mL^{-1}) for 4 h. Lastly, the supernatant in the 96-well plate was aspirated and 150 μL DMSO was added and shaken for 10 min. Then the absorbance at 490 nm was measured with a microplate reader and cell viability was estimated by $A/A_0 \times 100\%$ (A and A_0 are the absorbance of the experimental group and control group, respectively).

2.4. Confocal imaging in living cells

The HepG2 cells were cultured in laser confocal culture dishes at 37 °C for 24 h to ensure good cell growth and then washed three times with Dulbecco's phosphate buffered saline (DPBS). In a control experiment, HepG2 cells were pretreated with 1 mM *N*-methylmaleimide (sulfhydryl masking agent) for 40 min and washed three times with DPBS. Then HepG2 cells were

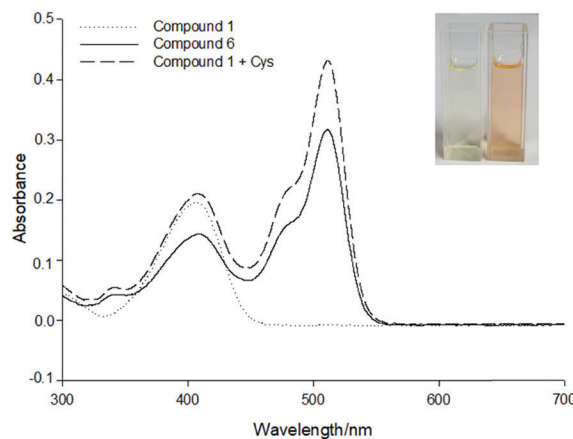


Fig. 3 Absorption spectra of fluorescent probe 1 (10 μM), compound 6 (10 μM), and the reaction mixture of fluorescent probe 1 (10 μM) with cysteine (100 μM). The dotted line (---), solid line (—), and dashed line (---) represent fluorescent probe 1, compound 6 and the reaction product of fluorescent probe 1 with cysteine, respectively. Inset: Color changes of probe 1 upon addition of cysteine.

incubated with 10 μM probe **1** for 45 min, rinsed with DPBS three times and imaged. In the experimental group of imaging endogenous Cys, HepG2 cells were treated with 10 μM probe **1** for 45 min, after which the cells were washed with DPBS three times and imaged. In the experimental group of imaging exogenous Cys, HepG2 cells were incubated with 10 μM probe **1** for 45 min and washed three times with DPBS, after which the cells were incubated with 0.1 mM Cys for another 45 min, washed three times with DPBS and imaged. Confocal fluorescence images were observed using an Olympus FV1200-MPE multiphoton confocal microscope with a 60 \times objective lens.

3. Results and discussion

3.1. Spectroscopic analytical performance of probe **1** towards Cys

In the presence of 100 μM cysteine, the probe can exhibit better fluorescence sensing for cysteine (Fig. S1, ESI[†]). So, 60% organic

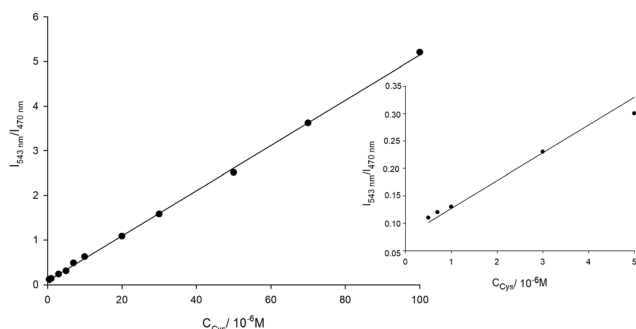
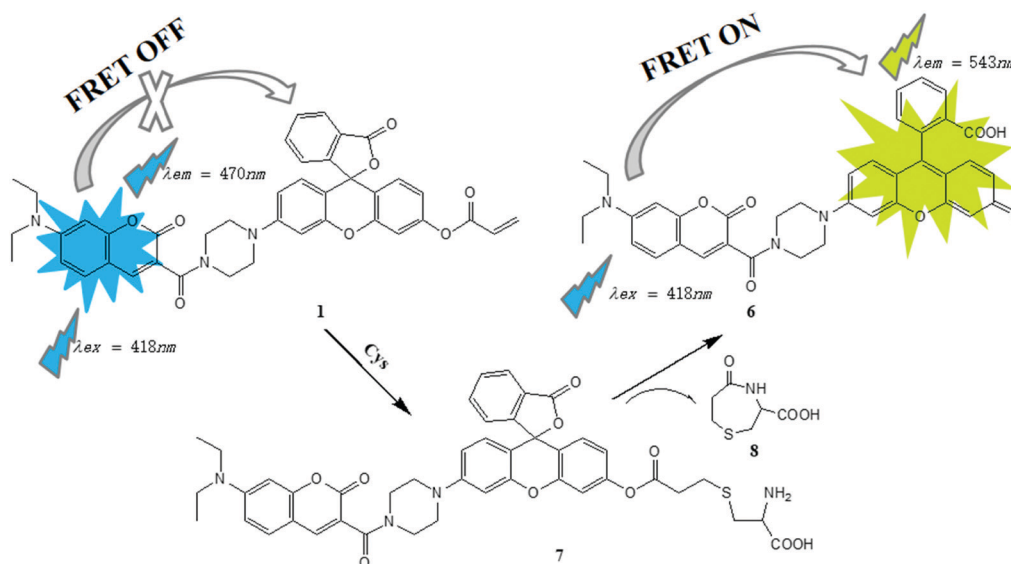


Fig. 4 Fluorescence intensity ratio ($I_{543\text{nm}}/I_{470\text{nm}}$) of probe **1** (10 μM) as a function of the concentration of cysteine from 0.5 μM to 100 μM . The inset exhibits the corresponding fluorescence intensity ratio ($I_{543\text{nm}}/I_{470\text{nm}}$) of probe **1** (10 μM) as a function of the concentration of cysteine from 0.5 μM to 5.0 μM .

solvents in buffer solution was used in the experiment. To study the fluorescence sensing properties of probe **1** for Cys, we investigated the change in fluorescence response of probe **1** (10 μM) to 0.01 M PBS buffer ($\text{CH}_3\text{CN}:\text{water} = 6:4$, v/v, pH = 7.40) containing different amounts of Cys (Fig. 2). From Fig. 2, when there is no cysteine, probe **1** exhibited strong fluorescence with an emission peak at 470 nm. However, in the presence of incremental Cys (0–100 μM), the initial fluorescence at 470 nm decreased gradually, and a new fluorescence emission peak appeared at 543 nm and increased progressively, permitting a ratiometric fluorescence response for Cys. It is remarkable that the large emission shift ($\Delta\lambda = 73$ nm) results in two well-resolved emission bands for the probe, which would be beneficial for dual-channel imaging of Cys in biological samples with less cross-talk observed. The notable change in fluorescence spectra should be attributed to Cys-induced occurrence of FRET between the donor coumarin and the acceptor rhodol. FRET efficiency is an important parameter of the FRET dye, which indicates the energy transfer efficiency between the donor and the acceptor. The fluorescence emission intensities of compound **5** (10 μM) and the reaction product of fluorescent probe **1** (10.0 μM) with cysteine (100 μM) at 470 nm were 8222 and 862 (Fig. S2, ESI[†]), so the fluorescence resonance energy transfer efficiency (ETE) = [(fluorescence of donor – fluorescence of donor in cassette)/fluorescence of donor] \times 100%.⁴⁸

We further studied the UV-Vis absorption spectra of probe **1** (10 μM), the reaction mixture of fluorescent probe **1** (10 μM) with cysteine (100 μM), and compound **6** (10 μM) (Fig. 3). From Fig. 3, probe **1** has a maximum absorption at 407 nm, which corresponds to the absorption of the coumarin donor,⁴⁹ and compound **6** absorbs at both 407 nm and 511 nm. In the presence of cysteine, no obvious changes in the absorption of the donor occurred, while a new absorption peak at 511 nm belonging to the conjugated xantheno form of the acceptor



Scheme 2 Proposed possible mechanism of the response of compound **1** to cysteine.

emerged.⁵⁰ The above results indicate that the reaction of the probe **1** with cysteine yields the compound **6**.

3.2. Principle of operation and the basis of quantitative assay

In order to investigate the linear response of the ratio value of the emission intensities at 543 nm and 470 nm ($I_{543\text{nm}}/I_{470\text{nm}}$) toward Cys, we chose different concentrations of Cys for experiments. When the concentration of cysteine was 5.0×10^{-7} – 1.0×10^{-4} mol L⁻¹ (Fig. 4), the ratio of $I_{543\text{nm}}/I_{470\text{nm}}$ was linear with the concentration of Cys. The linear regression equation was $I_{543\text{nm}}/I_{470\text{nm}} = 0.0763 + 0.0507 \times 10^6 \times C$ ($R = 0.9997$), where C is the concentration of cysteine and R is the linear correlation coefficient. The detection limit was calculated by $3S_B/m$, where S_B is the standard deviation of the fluorescence intensity measured 10 times for the blank solution

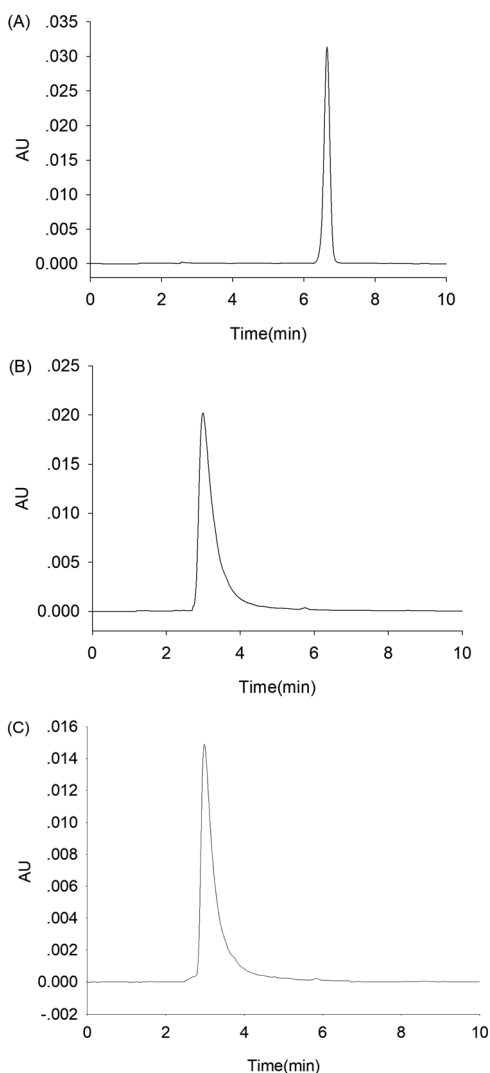


Fig. 5 HPLC profiles of (A) compound **1** (10 μM), (B) compound **6** (10 μM) and (C) the reaction mixture of compound **1** (10 μM) with cysteine (100 μM). HPLC conditions: 1.0 mL min⁻¹ total flow rate, Agela Technologies Venusil XBP-C18: 5 μm , 4.6×250 mm column, isocratic elution with acetonitrile at a flow rate of 0.8 mL min⁻¹ and water at a flow rate of 0.2 mL min⁻¹, detected at 407 nm.

and m is the slope of the calibration curve.⁴⁹ The detection limit of probe **1** for cysteine was 2.0×10^{-7} mol L⁻¹, which is much lower than that of a previously reported ratiometric fluorescent probe for Cys.^{46,51–53} The results indicate that probe **1** can be used for highly sensitive quantitative detection of cysteine.

The response mechanism of probe **1** to cysteine may be ascribed to the reaction of probe **1** with Cys to produce compound **6** (Scheme 2). As displayed in Scheme 2, in the absence of cysteine, the rhodol receptor was in the non-fluorescent lactone state and the FRET process was inhibited. Upon addition of cysteine, a Michael addition reaction took place between the acryloyl group of probe **1** and the thiol group of Cys to generate thioether compound **7**. Subsequently, compound **7** underwent an intramolecular cyclization to produce compound **6** accompanied by the release of the cyclization product **8**. Thus, in the presence of cysteine, the closed spirolactone form was converted to a conjugated fluorescent xanthene form to induce the occurrence of FRET. In order to further verify the reaction mechanism of probe **1** for cysteine, we performed HPLC on probe **1**, the reaction mixture of probe **1** with Cys and compound **6** (Fig. 5). As shown in Fig. 5, probe **1** showed a peak at 6.65 min, and the reaction mixture of probe **1** with cysteine showed a peak after 2.98 min of injection, which was consistent with the retention time of compound **6** in the HPLC. The ESI-MS data of the reaction mixture of probe **1** with Cys for 10 min displayed signals at 642.2215 and 819.0283, respectively (Fig. S3, ESI[†]). As illustrated in Fig. S3 (ESI[†]), the signal at 642.2215 was consistent with the structure [compound **6** – H]⁺ and the signal at 819.0283 was attributed to the structure [compound **7** + H]⁺. Simultaneously, in the ultraviolet absorption spectrum, the maximum absorption wavelengths of the compound **6** and the reaction mixture of probe **1** with cysteine were identical. Therefore, it can be proved that the response mechanism of probe **1** to cysteine was presumed to be correct.

3.3. Time-dependent responses and effect of pH

We further investigated the time dependent response of probe **1** (10 μM) under the conditions of addition of Cys (100 μM)

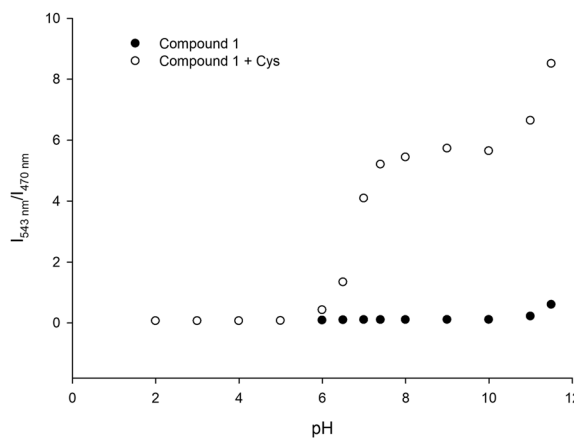


Fig. 6 Effect of pH on the ratio of fluorescence intensity ($I_{543\text{nm}}/I_{470\text{nm}}$) of 10 μM probe **1** in the absence (filled circles) and presence of 100 μM cysteine (clear circles). All data were obtained at various pH values (pH 2.00–11.50).

(Fig. S4, ESI[†]). Fig. S4 (ESI[†]) shows the trend of the value of $I_{543\text{nm}}/I_{470\text{nm}}$ over time. When Cys (100 μM) was added, the value continued to increase, reached a maximum and saturated at 60 min. The experimental results showed that probe **1** is stable under the experimental conditions, and the detection of cysteine can be completed within 60 min. In this study, an assay time of 60 min was chosen as the optimal measurement condition.

In order to test the sensitivity of the synthesized probe **1**, we studied the changes in the $I_{543\text{nm}}/I_{470\text{nm}}$ values of the synthesized probe **1** (10 μM) before and after adding Cys (100 μM) at different pH values (Fig. 6). As depicted in Fig. 6, the probe **1** has good sensitivity to Cys in a pH range of 6.00–11.50. Therefore, experimental results showed that probe **1** can work in a large pH range and can be used for biological detection.

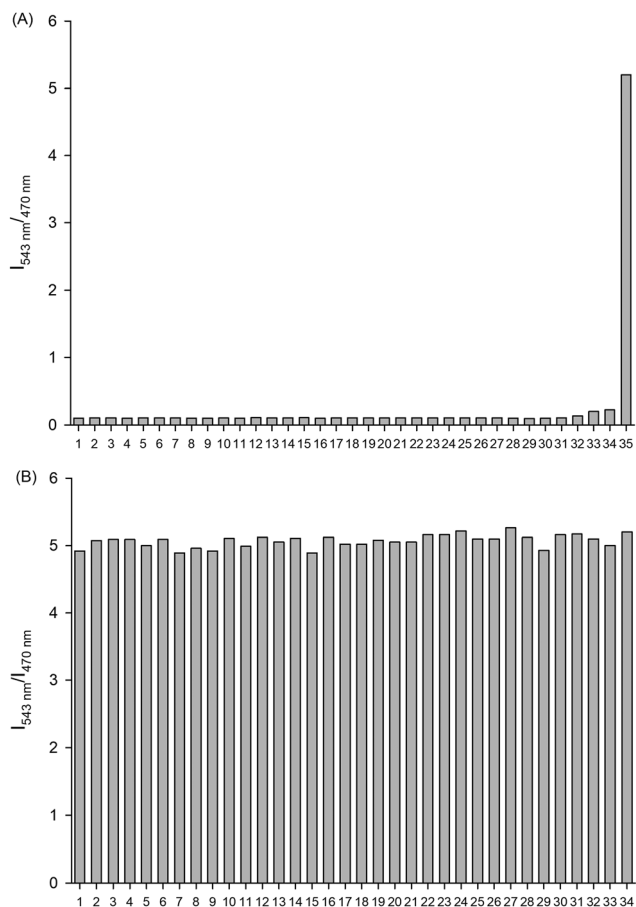


Fig. 7 (A) Fluorescence response of probe **1** (10 μM) toward Cys and other substances at pH 7.40: (1) blank, (2) Thr, (3) Leu, (4) Met, (5) Val, (6) Phe, (7) Ser, (8) Asn, (9) Trp, (10) Tyr, (11) Gln, (12) Lys, (13) Ile, (14) Ala, (15) His, (16) Asp, (17) Arg, (18) Pro, (19) Glu, (20) Gly, (21) F^- , (22) CO_3^{2-} , (23) CH_3COO^- , (24) $\text{S}_2\text{O}_3^{2-}$, (25) NO_2^- , (26) SO_4^{2-} , (27) Cl^- , (28) NO_3^- , (29) I^- , (30) Br^- , (31) SCN^- , (32) SO_3^{2-} , (33) Hcy, (34) GSH, and (35) Cys. (B) Fluorescence response of probe **1** (10 μM) toward Cys in the presence of other substances at pH 7.40: (1) Thr, (2) Leu, (3) Met, (4) Val, (5) Phe, (6) Ser, (7) Asn, (8) Trp, (9) Tyr, (10) Gln, (11) Lys, (12) Ile, (13) Ala, (14) His, (15) Asp, (16) Arg, (17) Pro, (18) Glu, (19) Gly, (20) F^- , (21) CO_3^{2-} , (22) CH_3COO^- , (23) $\text{S}_2\text{O}_3^{2-}$, (24) NO_2^- , (25) SO_4^{2-} , (26) Cl^- , (27) NO_3^- , (28) I^- , (29) Br^- , (30) SCN^- , (31) SO_3^{2-} , (32) Hcy, (33) GSH, and (34) Cys. The concentration of all substances added to probe **1** is 100 μM .

3.4. Selectivity

An important indicator for evaluating the performance of the fluorescent probe for target sensing is selectivity. We studied the fluorescence response of probe **1** to cysteine and other related substances at pH 7.40 (Fig. 7A). As shown in Fig. 7A, in the presence of cysteine probe **1** showed significant fluorescence enhancement, while the addition of other substances had little effect on the fluorescence of probe **1**. To investigate the potential applications of probes in complex biological samples, we also investigated the effect of coexistence of other substances and cysteine on the sensitivity of the fluorescent probe to cysteine at a pH of 7.40 (Fig. 7B). From Fig. 7B, the probe still maintained a fluorescence response to cysteine in the presence of other related substances.

3.5. Cytotoxicity assays and confocal imaging in living cells

We tested the cytotoxicity of probe **1** and compound **6** at different concentrations (0, 2, 4, 8, and 16 μM) against HepG2 cells by MTT assay (Fig. 8). As depicted in Fig. 8, when probe **1** and compound **6** were present, cell viability reached 80% or more, which indicates that probe **1** and compound **6** were almost non-toxic to HepG2 cells.

In order to demonstrate the practicality of probe **1** in biological detection, we performed laser confocal fluorescence imaging of

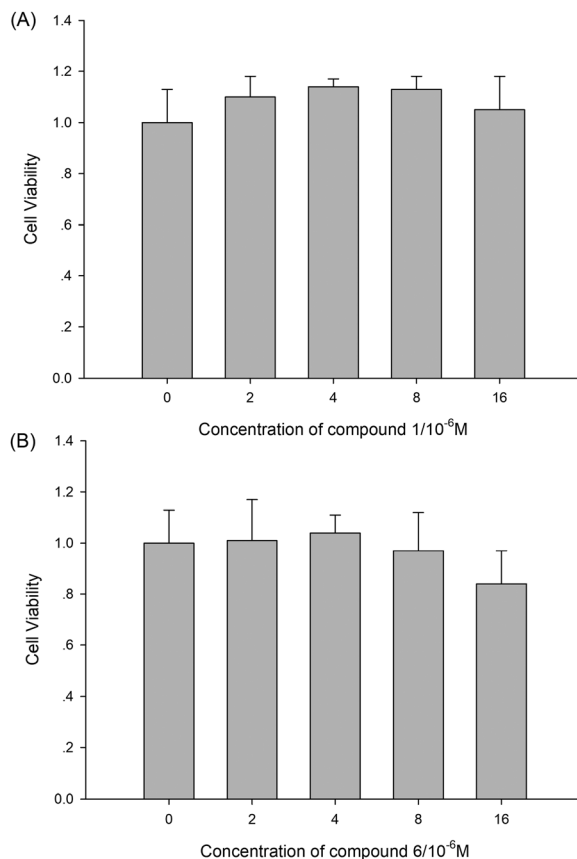


Fig. 8 MTT assay of HepG2 cells in the presence of different concentrations of compound **1** (A) and compound **6** (B) (0, 2, 4, 8, and 16 μM) for 24 h at 37 $^\circ\text{C}$, respectively.

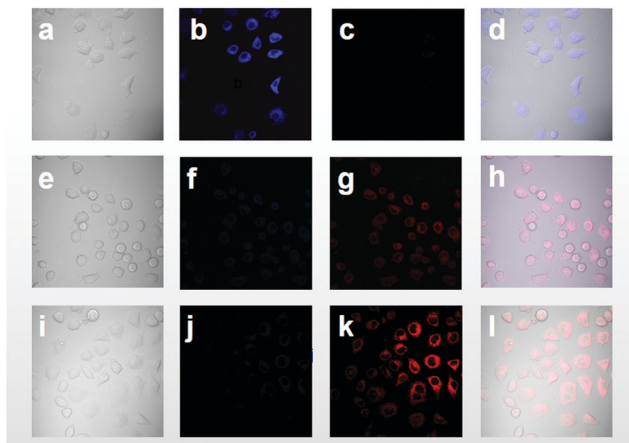


Fig. 9 Laser confocal fluorescence imaging of cysteine in HepG2 cells with fluorescent probe **1**. (a) Bright field image after incubation of HepG2 cells with 1 mM *N*-methylmaleimide for 40 min and incubation of HepG2 cells with 10 μ M probe **1** for 45 min; (b) fluorescence image from the blue channel of image (a); (c) fluorescence image from the red channel of image (a); (d) overlay image of (a–c); (e) bright field map after incubation of HepG2 cells with 10 μ M probe **1** for 45 min; (f) fluorescence image from the blue channel of image (e); (g) fluorescence image from the red channel of image (e); (h) overlay image of (e–g); (i) bright field images of HepG2 cells incubated with probe **1** for 45 min and then with 10 μ M Cys for 45 min; (j) fluorescence image from the blue channel of image (i); (k) fluorescence image from the red channel of image (i); (l) overlay image of (i–k).

cysteine in HepG2 cells with fluorescent probe **1** (Fig. 9). HepG2 cells were seeded in three 35 mm laser confocal culture dishes and incubated for 24 h. The HepG2 cells were pretreated with 1 mM *N*-methylmaleimide (sulfhydryl masking agent) for 40 min, and incubated in a medium containing 10 μ M probe **1** for 45 min for fluorescence imaging. It was found that the blue channel has obvious fluorescence (Fig. 9b), and the red channel has almost no fluorescence (Fig. 9c). In the control experiment, HepG2 cells were incubated in a medium containing 10 μ M probe **1** for 45 min for fluorescence imaging. The results showed that the blue channel showed weak fluorescence (Fig. 9f) and the red channel showed more obvious fluorescence (Fig. 9g). Simultaneously, HepG2 cells were incubated with 10 μ M probe **1** for 45 min, then incubated with 0.1 mM Cys for 45 min and imaged. The experimental results showed that the fluorescence of the blue channel was weak (Fig. 9j), and the fluorescence of the red channel was stronger than that without added Cys (Fig. 9k). These phenomena indicate that the probe **1** can be used for the ratiometric dual-channel detection of cysteine in living cells.

4. Conclusions

In summary, we designed and synthesized a FRET-based ratiometric probe for detection of Cys based on a coumarin–rhodol derivative. An acrylate group was applied as an identification group for Cys. In the absence of cysteine, the rhodol receptor was in the non-fluorescent lactone state and the FRET process was inhibited. Upon addition of cysteine, the closed spiro lactone

form was converted to a conjugated fluorescent xanthene form to induce the occurrence of FRET which resulted in a fluorescent signal decrease at 470 nm and enhancement at 543 nm. The probe shows high sensitivity and selectivity for cysteine over glutathione, homocysteine, and other related substances. In addition, the probe also has good cell permeability and has been successfully applied for the ratiometric dual-channel detection of cysteine in living cells.

Conflicts of interest

There are no conflicts of interest to declare.

Acknowledgements

This work was supported by the Key Science and Technology Programme of Henan Province (182102310101), the National Natural Science Foundation of China (Grant no. 21807027 and 81130062), the Fundamental Research Funds for the Provincial Universities (2014KYYWF-QN04), and the Graduate Innovation Fund in Henan College of Chinese Medicine (YJS2018A05).

References

- 1 X. Chen, Y. Zhou, X. Peng and J. Yoon, *Chem. Soc. Rev.*, 2010, **39**, 2120.
- 2 Y. Yang, Q. Zhao, W. Feng and F. Li, *Chem. Rev.*, 2013, **113**, 192.
- 3 D. M. Townsend, K. D. Tew and H. Tapiero, *Biomed. Pharmacother.*, 2003, **57**, 145.
- 4 K. G. Reddie and K. S. Carroll, *Curr. Opin. Chem. Biol.*, 2008, **12**, 746.
- 5 E. Weerapana, C. Wang, G. M. Simon, M. B. D. Dillon, D. A. Bachovchin, K. Mowen, D. Baker and B. F. Cravatt, *Nature*, 2010, **468**, 790.
- 6 A. K. Elshorbagy, V. Kozich, A. D. Smith and H. Refsum, *Curr. Opin. Clin. Nutr. Metab. Care*, 2012, **15**, 49.
- 7 M. T. Heafield, S. Fearn, G. B. Steventon, R. H. Waring, A. C. Williams and S. G. Sturman, *Neurosci. Lett.*, 1990, **110**, 216.
- 8 R. Janáky, V. Varga, A. Hermann, P. Saransaari and S. S. Oja, *Neurochem. Res.*, 2000, **25**, 1397.
- 9 X. F. Wang and M. S. Cynader, *J. Neurosci.*, 2001, **21**, 3322.
- 10 W. Zhang, P. Li, Q. Geng, Y. Duan, M. Guo and Y. Cao, *J. Agric. Food Chem.*, 2014, **62**, 5845.
- 11 Y. Wang, C. H. Zhang, Y. H. Zheng, Y. Ge and X. Y. Yu, *Anal. Lett.*, 2019, **52**, 1487.
- 12 A. V. Ivanov, E. D. Virus, B. P. Luzyanin and A. A. Kubatiev, *J. Chromatogr. B: Anal. Technol. Biomed. Life Sci.*, 2015, **1004**, 30.
- 13 R. C. de Carvalho, T. R. D. Mathias, A. D. P. Netto and F. F. D. Marques, *Electrophoresis*, 2018, **39**, 1613.
- 14 N. Shao, J. Y. Jin, S. M. Cheung, R. H. Yang, W. H. Chan and T. Mo, *Angew. Chem.*, 2006, **118**, 5066.

- 15 Y. Sato, T. Iwata, S. Tokutomi and H. Kandori, *J. Am. Chem. Soc.*, 2005, **127**, 1088.
- 16 Y. Zhou and J. Yoon, *Chem. Soc. Rev.*, 2012, **41**, 52.
- 17 X. Chen, T. Pradhan, F. Wang, J. S. Kim and J. Yoon, *Chem. Rev.*, 2012, **112**, 1910.
- 18 X. Yang, Y. Guo and R. M. Strongin, *Angew. Chem., Int. Ed.*, 2011, **50**, 10690.
- 19 L. He, B. Dong, Y. Liu and W. Lin, *Chem. Soc. Rev.*, 2016, **45**, 6449.
- 20 L. Y. Niu, Y. Z. Chen, H. R. Zheng, L. Z. Wu, C. H. Tung and Q. Z. Yang, *Chem. Soc. Rev.*, 2015, **44**, 6143.
- 21 Z. L. Lu, Y. N. Lu, C. H. Fan, X. Sun, W. Q. Shao, N. Jiang, X. Y. Gong, Y. Z. Lu, G. X. Sun and X. C. Jiang, *Sens. Actuators, B*, 2019, **290**, 581.
- 22 D. J. Zhu, X. W. Yan, A. S. Ren, W. Xie and Z. H. Duan, *Anal. Chim. Acta*, 2019, **1058**, 136.
- 23 P. Srivastava, R. C. Gupta and A. Misra, *ChemistrySelect*, 2018, **3**, 12900.
- 24 J. Li, Y. k. Yue, F. J. Huo and C. X. Yin, *Dyes Pigm.*, 2019, **164**, 339.
- 25 W. Zhang, X. Y. Zhao, W. J. Gu, T. Cheng, B. X. Wang, Y. L. Jiang and J. Shen, *New J. Chem.*, 2018, **42**, 18109.
- 26 S. Jiao, X. He, L. B. Xu, P. Y. Ma, C. M. Liu, Y. B. Huang, Y. Sun, X. H. Wang and D. Q. Song, *Sens. Actuators, B*, 2019, **290**, 47.
- 27 Z. L. Lu, Y. N. Lu, C. H. Fan, X. Sun, W. Q. Shao, N. Jiang, X. Y. Gong, Y. Z. Lu, G. X. Sun and X. C. Jiang, *Sens. Actuators, B*, 2019, **290**, 581.
- 28 D. G. Chen, Z. Long, Y. C. Dang and L. Chen, *Dyes Pigm.*, 2019, **166**, 266.
- 29 K. S. Lee, T. K. Kim, J. H. Lee, H. J. Kim and J. I. Hong, *Chem. Commun.*, 2008, 6173.
- 30 Z. G. Yang, N. Zhao, Y. M. Sun, F. Miao, Y. Liu, X. Liu, Y. H. Zhang, W. T. Ai, G. F. Song, X. Y. Shen, X. Q. Yu, J. Z. Sun and W. Y. Wong, *Chem. Commun.*, 2012, **48**, 3442.
- 31 M. J. Wei, P. Yin, Y. M. Shen, L. L. Zhang, J. H. Deng, S. Y. Xue, H. T. Li, B. Guo, Y. Y. Zhang and S. Z. Yao, *Chem. Commun.*, 2013, **49**, 4640.
- 32 W. S. Qua, L. Yang, Y. D. Hang, X. Zhang, Y. Qu and J. L. Hua, *Sens. Actuators, B*, 2015, **211**, 275.
- 33 X. F. Hou, Z. S. Li, B. L. Li, C. H. Liu and Z. H. Xu, *Sens. Actuators, B*, 2018, **260**, 295.
- 34 Y. Tian, B. C. Zhu, W. Yang, J. Jing and X. L. Zhang, *Sens. Actuators, B*, 2018, **262**, 345.
- 35 H. Fang, N. Wang, L. Xie, P. C. Huang, K. Y. Deng and F. Y. Wu, *Sens. Actuators, B*, 2019, **294**, 69.
- 36 L. H. Liu, Q. Zhang, J. Wang, L. L. Zhao, L. X. Liu and Y. Lu, *Talanta*, 2019, **198**, 128.
- 37 X. Y. He, X. F. Wu, W. Shi and H. M. Ma, *Chem. Commun.*, 2016, **52**, 9410.
- 38 H. J. Xiang, H. P. Tham, M. D. Nguyen, S. Z. F. Phua, W. Q. Lim, J. G. Liu and Y. L. Zhao, *Chem. Commun.*, 2017, **53**, 5220.
- 39 L. H. Zhai, Z. L. Shi, Y. Y. Tu and S. Z. Pu, *Dyes Pigm.*, 2019, **165**, 164.
- 40 J. Li, Y. Yue, F. Huo and C. Yin, *Dyes Pigm.*, 2019, **164**, 335.
- 41 B. Dong, Y. Lu, N. Zhang, W. Song and W. Zhang, *Anal. Chem.*, 2019, **91**, 5513.
- 42 D. Zhu, X. Yan, A. Ren, W. Xie and Z. Duan, *Anal. Chim. Acta*, 2019, **1058**, 136.
- 43 X. Li, H. Ma, J. Qian, T. Cao, Z. Teng, K. Iqbal, W. Qin and H. Guo, *Talanta*, 2019, **194**, 717.
- 44 W. Xuan, Y. Cao, J. Zhou and W. Wang, *Chem. Commun.*, 2013, **18**, 10474.
- 45 K. Huang, M. Liu, Z. Liu, D. Cao, J. Hou and W. Zeng, *Dyes Pigm.*, 2015, **118**, 88.
- 46 L. He, X. Yang, K. Xu and W. Lin, *Anal. Chem.*, 2017, **89**, 9567.
- 47 S. Yang, C. Guo, Y. Li, J. Guo, J. Guo, J. Xiao, Z. Qing, J. Li and R. Yang, *ACS Sens.*, 2018, **3**, 2415.
- 48 J. Zhang, X. Y. Zhu, X. X. Hu, H. W. Liu, J. Li, L. L. Feng, X. Yin, X. B. Zhang and W. H. Tan, *Anal. Chem.*, 2016, **88**, 11892.
- 49 K. Huang, L. Yu, P. Xu, X. Zhang and W. Zeng, *RSC Adv.*, 2015, **5**, 17797.
- 50 X. Zhu, M. Xiong, H. Liu, G. Mao, L. Zhou, J. Zhang, X. Hu, X. B. Zhang and W. Tan, *Chem. Commun.*, 2016, **52**, 733.
- 51 J. Li, Y. Yue, F. Huo and C. Yin, *Dyes Pigm.*, 2019, **164**, 335.
- 52 B. Dong, Y. Lu, N. Zhang, W. Song and W. Lin, *Anal. Chem.*, 2019, **91**, 5513.
- 53 L. Fan, W. Zhang, X. Wang, W. Dong, Y. Tong, C. Dong and S. Shuang, *Analyst*, 2019, **144**, 439.